Molecular Crystals and Liquid Crystals

Publication details, including instructions for authors and subscription information:
http://www.tandfonline.com/loi/gmcl20

Effect of Slow Cooling on a Discotic Nematic Liquid Crystal: Evidences for Nematic-Nematic Transitions

D. Vijayaraghavan [a] & Sandeep Kumar [a]

[a] Raman Research Institute, Sadashivanagar, Bangalore, India

Version of record first published: 31 Aug 2006

To cite this article: D. Vijayaraghavan & Sandeep Kumar (2006): Effect of Slow Cooling on a Discotic Nematic Liquid Crystal: Evidences for Nematic-Nematic Transitions, Molecular Crystals and Liquid Crystals, 452:1, 11-26

To link to this article: http://dx.doi.org/10.1080/15421400500377636

Mol. Cryst. Liq. Cryst., Vol. 452, pp. 11–26, 2006

ISSN: 1542-1406 print/1563-5287 online
DOI: 10.1080/15421400500377636

Taylor & Francis
Taylor & Francis Group

Effect of Slow Cooling on a Discotic Nematic Liquid Crystal: Evidences for Nematic–Nematic Transitions

D. Vijayaraghavan
Sandeep Kumar
Raman Research Institute, Sadashivanagar, Bangalore, India

There is considerable interest in discotic liquid crystals because of their possible applications in liquid crystal displays and in one-dimensional conductors. In view of these applications, knowledge and control of their phase behavior and transition temperatures are crucial. We have studied a discotic nematic liquid crystal, namely, hexakis(4-nonylphenylethynyl)benzene. The phase sequence reported for this sample on cooling is isotropic (I) 81.8°C discotic nematic (N_D) and 39°C crystal (Cr). The phase sequences were obtained using differential scanning calorimetry (DSC) and optical polarizing microscopy (OPM) studies while varying the sample temperature rapidly (5°C/min). However, on slowly cooling the sample (0.36°C/min), we observed anomalous optical textures and DSC peaks in the nematic region at 75°C and 52°C. We also find discontinuous changes in the optical transmission intensity and diamagnetic anisotropy in the vicinity of these temperatures on slow cooling. Further, the XRD pattern showed small but distinct shifts in the lateral (100) peaks in the vicinity of these transitions. We infer that the variations in the lateral distance between the discotic molecules may be responsible for these observed nematic–nematic (N-N) transitions.

Keywords: discotic nematic; nematic–nematic transitions

1. INTRODUCTION

Discotic liquid crystals exhibit various mesophases. Columnar mesophases are obtained if the disk-shaped mesogens stack into columns possessing a long-range two-dimensional (2D) order. Besides highly ordered columnar phases, they exhibit different nematic phases. In the nematic discotic phase (N_D), the mesogens only possess orientational order. In the nematic columnar phase (N_{col}), the molecules stack into short columns, and the columns order in a nematic arrangement,

Address correspondence to D. Vijayaraghavan, Raman Research Institute, C. V. Raman Avenue, Sadashivanagar, Bangalore 560 080, India. E-mail: vijay@rri.res.in

analogous to the nematic phase in calamitic liquid crystals. Depending on the system, various mechanisms such as charge transfer, steric interactions, or even the restricted mobility of the disk-like molecules are found to be responsible for the occurrence of these nematic columnar phases [1–3]. Recently, another novel nematic lateral (N_L) phase was reported in a charge transfer complex of an electron-rich discotic molecule and an electron-deficient acceptor macromolecule [4,5].

Hexaalkynylbenzene derivatives with an N_D phase have recently received a great deal of attention as their clearing temperatures are not very high and they can be easily aligned on commercially available glass cells. Moreover, no coating of the glass plates is required to achieve a good homeotropic alignment of the director [6–8]. Several hexaalkynylbenzenes have been prepared and studied extensively. Efforts have been made to stabilize the discotic nematic phase of these materials at ambient temperature by changing peripheral substitutions [9–11]. Hexakis(4-nonylphenylethynyl)benzene (**6**) is a unique substance that forms a discotic nematic phase at moderate temperatures ranging from 68 to 83°C [12]. Upon cooling the isotropic phase, the nematic phase appears at 81.8°C, which crystallizes at about 39°C [13]. Chandrasekhar and coworkers have recently used this discotic nematic liquid crystal instead of commonly used calamitic nematic liquid crystals to improve the viewing angle of a liquid crystal display device [13]. This compound is also known to form novel chiral nematic–discotic phases upon doping with suitable chiral molecules [12,14].

On slowly cooling our nematic liquid crystal sample, hexakis(4-nonylphenylethynyl) benzene, we observed anomalous changes in the nematic region in our thermal, optical, magnetic, and x-ray studies. We may attribute these changes to nematic–nematic transitions brought about by the variations in the lateral distance between the discotic molecules. Here, we report our thermal, optical, and magnetic studies of a discotic nematic liquid crystal, namely hexakis(4-nonylphenyl ethynyl)benzene, upon slow cooling.

2. EXPERIMENTAL

2.1. Synthesis

Hexakis(4-nonylphenylethynyl)benzene (**6**) was prepared following the procedure reported earlier [9], and the scheme is shown in Fig. 1. Commercially available nonanoic acid is converted to its acid chloride using oxalyl chloride at room temperature. Friedel–Crafts acylation of the bromobenzene (**1**) with the acid chloride gives the

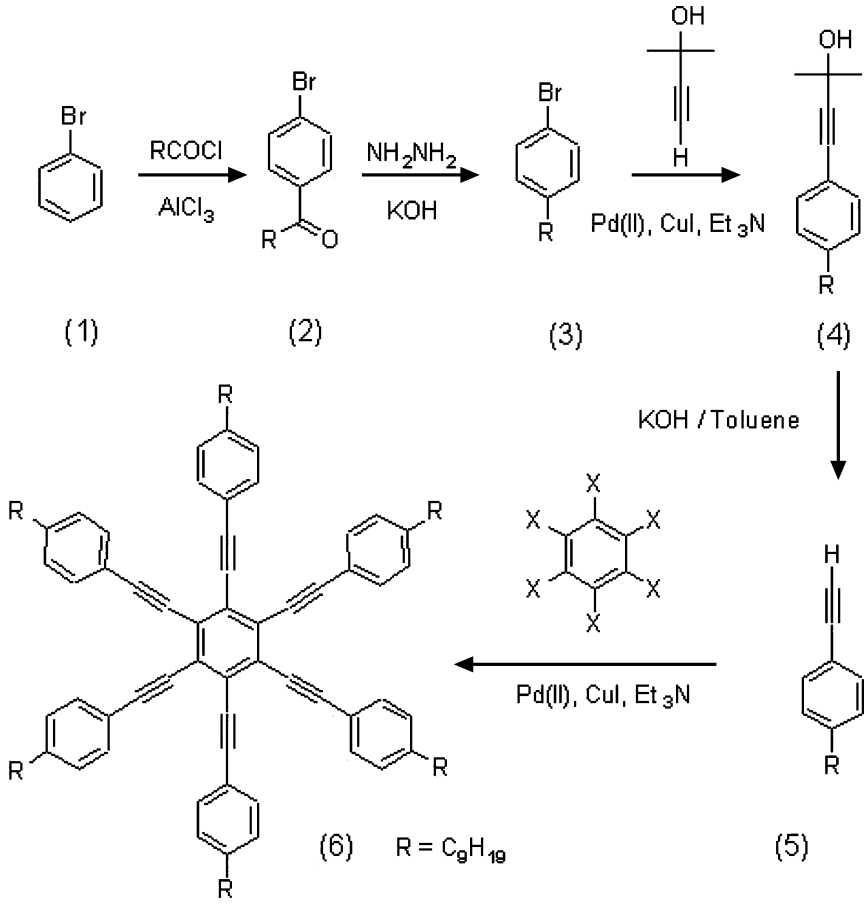

FIGURE 1 Schematic of the synthesis of the compound hexakis(4-nonylphenylethynyl)benzene.

1-bromo-4-nonanoylbenzene **2**. Wolff–Kishner reduction of the ketone **2** furnished 1-bromo-4-nonylbenzene **3**. Pd-catalyzed alkynylation of **3** with 2-methyl-3-butyn-2-ol afforded the protected phenylacetylene **4**, which was deprotected using KOH in refluxing toluene to yield the phenylacetylene **5**. A palladium-catalyzed coupling of this phenylacetylene **5** with hexabromobenzene yielded the desired hexakis (4-nonylphenylethynyl)benzene **6**. The compounds are purified by repeated column chromatography, followed by crystallization with an ether–methanol mixture and characterized from spectral analysis, thermal behavior, and direct comparison with an authentic sample.

2.2. X-ray Studies

X-ray studies were carried out using a rotating anode generator operating at 48 KV, 80 mA (Rigaku Ultra $\times 18$). CuKα radiation was selected using a flat graphite (Huber) monochromator. Diffraction patterns are recorded on a 2D image plate detector (Marresearch) 180 mm in diameter. The sample is filled in a glass capillary 1 mm in diameter and flame sealed. The sample is kept in a magnetic field of $\sim$1 kilo Gauss. The sample temperature is controlled using a computer-controlled temperature controller. The sample is heated slowly to the isotropic temperature, and the diffraction data is collected while slowly cooling the sample (0.36°C/min).

2.3. Thermal and Morphological Studies

The sample is studied by differential scanning calorimetry (DSC) and optical polarizing microscopy (OPM). Thermal properties of the sample are studied using a Perkin-Elmer DSC-7 instrument under N_2 gas flow. Two indium tin oxide (ITO)-coated glass plates are sandwiched using a 6-μm Mylar® spacer, and the cell is filled when the sample is in the isotropic phase. Morphological studies are carried out on the 6-μm sample using a Leitz polarizing optical microscope equipped with a Mettler hot stage FP-82.

2.4. Magnetic Susceptibility Studies

The magnetic susceptibility studies are carried out using a Faraday balance. A schematic diagram of the experimental setup is shown in Fig. 2. A continuous flow cryostat (CF 1200, Oxford Instruments) is held between the pole pieces of an electromagnet (Oxford Instruments). The pole tips are shaped to give a constant value of H_x (dH_x/dH_z) in the sample region of about $15 \times 12 \times 12\,mm^3$ (where H_x refers to the magnetic field strength of 11 kiloGauss and dH_x/dH_z is the magnetic filed gradient at the sample region). The sample is suspended from the sample port of a Sartorius balance (model SD3V), which has a resolution of 0.1 μg and has a maximum of 3 g through a 100-μm-thick quartz fiber. Initially, the susceptibility of an empty DSC cup (χ_{cup}) is measured by making the cup into a pan by using two small copper wires and hooking it to the fiber. The compensating weights are added in the weighing pan so that the reading on the balance is nearly zero in the absence of the magnetic field (M_o). The magnetic field is now applied, and the balance reading (M_c) is taken. The difference between these two values $M_c - M_o$ ($=\Delta M_c$) is related to the susceptibility through the equation $\Delta M_c g = \chi_{cup} m H_x (dH_x/dH_z)$, where

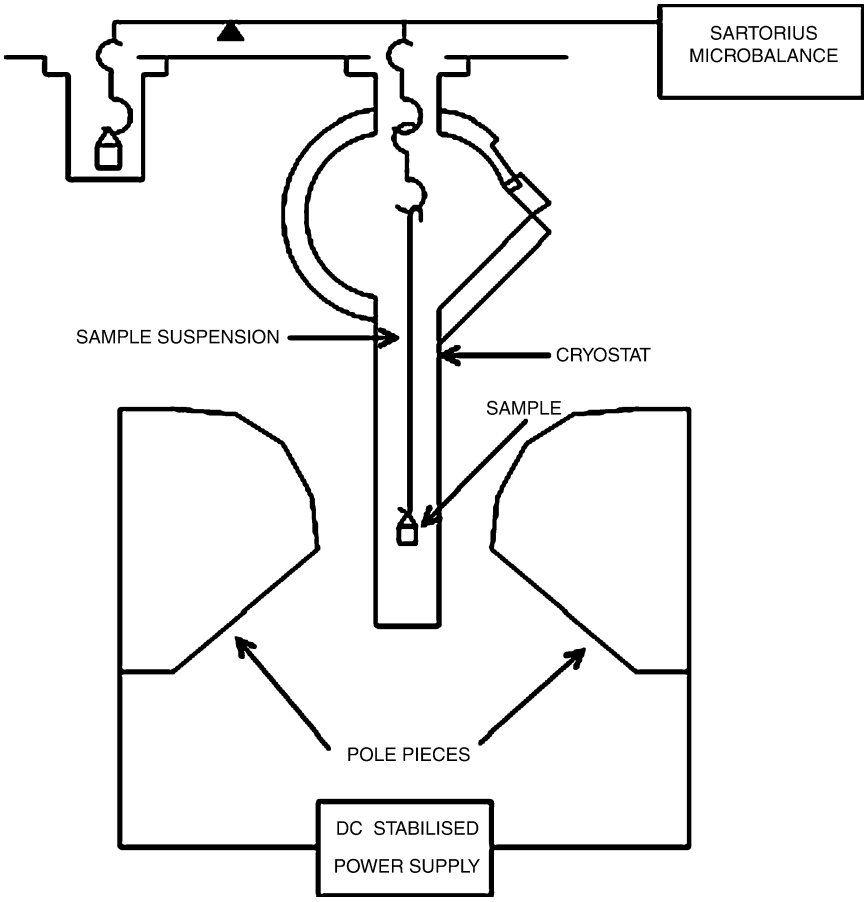

FIGURE 2 Schematic diagram of the experimental setup used in the magnetic susceptibility measurements.

g is the acceleration due to gravity (980 cm/s^2) and m is the mass of the sample. Then, the sample (about 10 mg) is filled in the DSC sample cup, and, after sealing placed on the pan, the susceptibility of the total system (χ_{total}) is measured as before. By using the relation

$$\chi_{\text{total}} m_{\text{total}} = \chi_{\text{cup}} m_{\text{cup}} + \chi_{\text{sample}} m_{\text{sample}}$$

we can measure the susceptibility of the sample (χ_{sample}). (Here, m_{cup} refers to the total mass of the pan and the empty DSC cup and m_{sample} refers to the mass of the sample.) Measurements are made by heating the sample to isotropic temperature and cooling it slowly in the

presence of the magnetic field. A chromel-alumel thermocouple is used to measure the temperature of the sample. The system is calibrated using 5CB, and the data is found to agree well with that reported in the literature [15]. In a similar way, the susceptibility measurements are carried out for the sample reported in this article. The sample is heated slowly at 0.6°C/min to about 5°C above the isotropic temperature, and the measurements are taken on second cooling of the sample while varying the sample temperature at 0.36°C/min.

2.5. Optical Transmission Studies

We have carried out optical transmission studies on a 6-μm sample. Two ITO-coated glass plates are sandwitched using a 6-μm spacer. This cell is filled when the sample is in the isotropic phase and is mounted in a heater arrangement consisting of a set of ITO-coated glass plates. The temperature of the sample is controlled using a computer-controlled temperature controller, the stability being about 10 mK. A platinum resistance thermometer placed close to the sample is used to measure the sample temperature accurately. The light beam from a He-Ne laser passes through a polariser and is incident on the sample. Then it passes through an analyser, which is crossed with respect to the polariser. The transmitted intensity as a function of temperature is measured by a photodiode with a built-in amplifier. The sample is heated slowly at 0.6°C/min to about 5°C above the isotropic temperature, and the measurements are taken on second cooling of the sample, while varying the sample temperature at 0.36°C

3. RESULTS AND DISCUSSION

The heat flow as a function of temperature (DSC thermogram) for the fast cooling (5°C/min) of the sample is shown in Fig. 3. The weak high temperature peak at 81°C is due to the isotropic (I) to discotic nematic (ND) transition (latent heat of transition ($\Delta H = 0.137\,\mathrm{Jg}^{-1}$) and the low temperature peak at 39°C is due to the nematic to crystal (Cr) transition ($\Delta H = 15\,\mathrm{Jg}^{-1}$). The texture of the fast-cooled sample is shown in the inset of Fig. 3. It shows the usual schlieren texture expected for a nematic phase.

However, on slow cooling (0.36°C/min), the DSC thermogram shows a different behavior, as shown in Fig. 4. It shows a broad exothermic peak at 75°C ($\Delta H = 8\,\mathrm{Jg}^{-1}$) and a weak endothermic peak at 52°C ($\Delta H = 5\,\mathrm{Jg}^{-1}$). It also shows a slope change at about 81°C and a sharp peak at 39°C ($\Delta H = 14\,\mathrm{Jg}^{-1}$), which correspond to isotropic and crystalline peaks respectively.

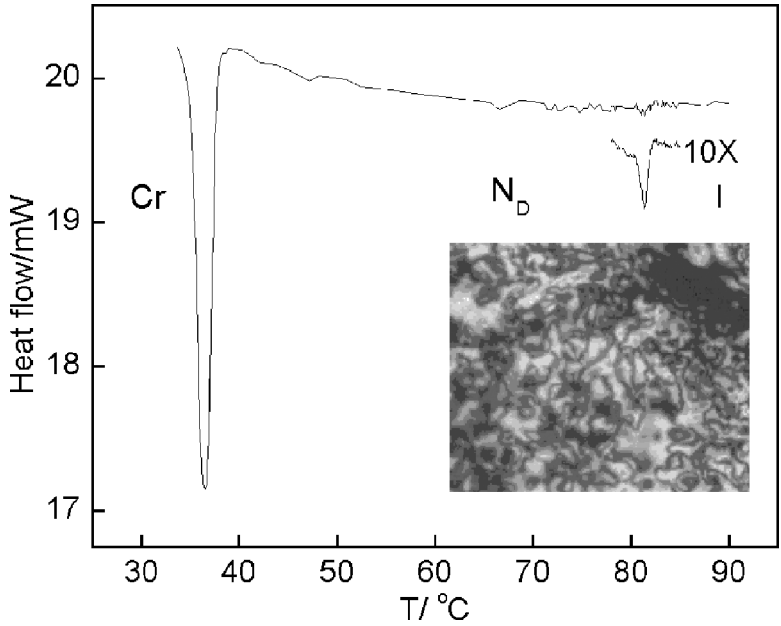

FIGURE 3 DSC thermogram for the fast cooling of the sample (5°C/min). The inset shows the optical texture.

The optical textures of the sample on slow cooling at different temperatures are shown in Fig. 5. Below the isotropic temperature, the sample exhibits marble texture along with nematic brushes. At 75°C only a marble texture is seen. The texture persists at lower temperatures with a gradual variation in the intensity. At 52°C, the marble texture changes to complementary colours. At 39°C, it shows crystalline texture. Nematic marble texture is usually observed in thin preparations of samples, especially for substrates that have not been rubbed or treated in any way [16].

Optical transmitted intensity studies are often used to probe phase transitions in liquid crystals [17,18]. We measured the optical transmitted intensity as a function temperature while slowly cooling the sample (Fig. 6). We find discontinuous changes at 75°C and 52°C in transmitted intensity, indicating a possible nematic–nematic transitions at these temperatures.

The diamagnetic susceptibility of the sample is measured as a function of temperature, and the diamagnetic anisotropy values are derived using the work of Levelut and Hardouin on a discotic nematic liquid crystal [19]. The diamagnetic susceptibility measured in the

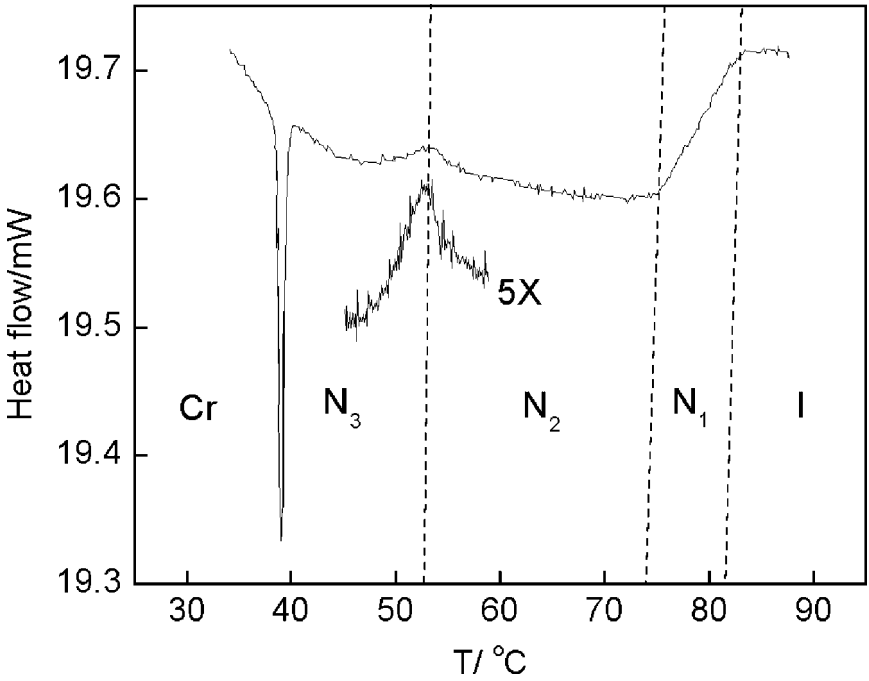

FIGURE 4 DSC thermogram for the slow cooling of the sample (0.36°C/min).

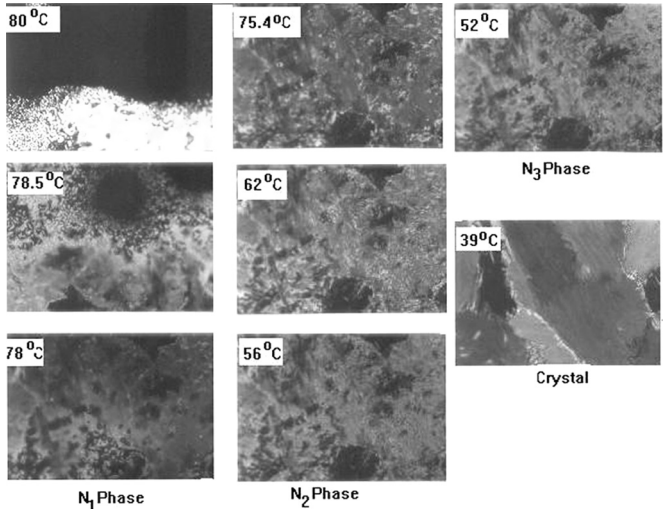

FIGURE 5 Optical textures of the sample on slow cooling at different temperatures.

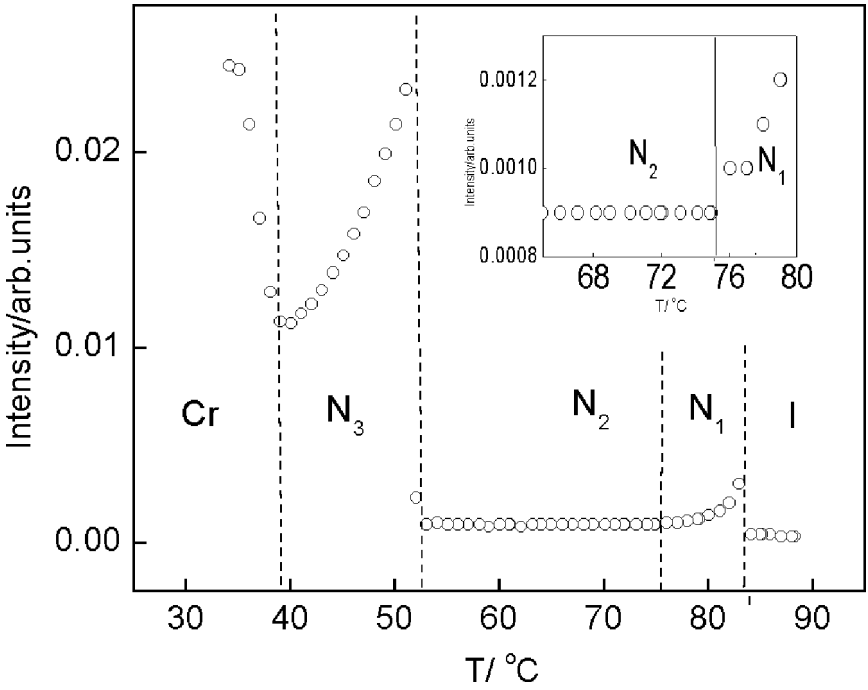

FIGURE 6 Optical transmitted intensity as a function of temperature on slow cooling of the sample (0.36°C/min).

direction of the static magnetic field by the Faraday method corresponds to the susceptibility perpendicular to the director (i.e., $\chi_\perp$). Then, the diamagnetic anisotropy is given by $\Delta\chi = \chi_\parallel - \chi_\perp = 3(\overline{\chi}_{\text{isotropic}} - \chi_\perp)$ where, $\overline{\chi}_{\text{isotropic}} = (2\chi_\perp + \chi_\parallel)/3$. In the experiment, $\overline{\chi}_{\text{isotropic}}$ refers to the temperature independent susceptibility measured in the isotropic phase, and $\chi_\perp$ refers to the susceptibility measured in the nematic phase. Figure 7 shows the diamagnetic anisotropy as a function of temperature on slow cooling of the sample. We find discontinuous changes in the diamagnetic anisotropy values at 75°C and 52°C indicating N-N transitions.

Figure 8 shows the X-ray diffraction (XRD) pattern of the sample on slow cooling for three different temperatures: 80°C, 70°C, and 50°C. The sharp peaks at the lower theta values correspond to the reflections in the lateral (100) direction, and the broad peaks at higher theta values correspond to reflections in the columnar (001) direction. The observed XRD patterns are comparable to those of reported discotic nematic liquid crystals [4,5]. Figures 8 and 9 show a small but distinct shift in the lateral peaks.

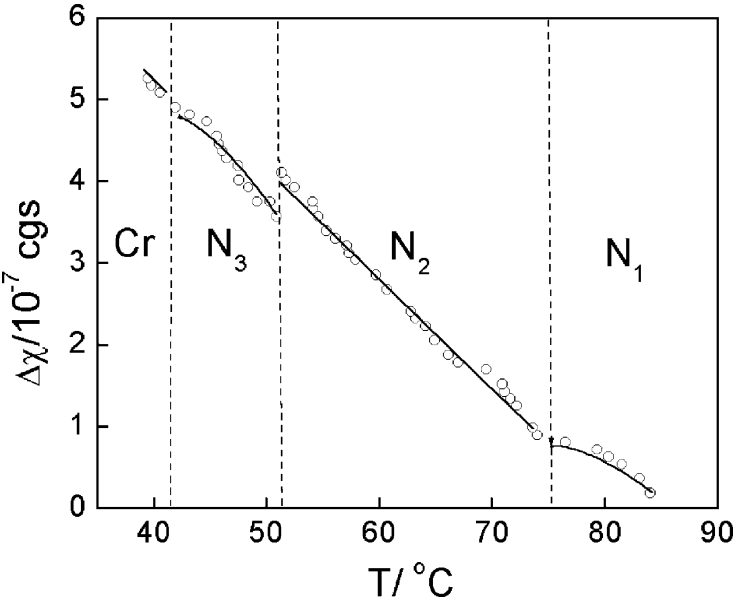

FIGURE 7 Diamagnetic anisotropy ($\Delta\chi$) as a function of temperature (T/°C) on slow cooling of the sample (0.36°C/min). Solid lines are guide to the eyes.

From our studies, we infer that the sample on slow cooling exhibits three nematic phases, N_1, N_2, and N_3. The high-temperature N_1 phase exists below isotropic temperature down to 75°C. The intermediate nematic phase N_2 exists between 75 and 52°C, and below 52°C, the N_3 phase exists. The sample crystallizes at 39°C. The latent heat values observed for N_1 to N_2 transition and for N_2 to N_3 transitions are $8\,Jg^{-1}$ and $5\,Jg^{-1}$ respectively. These values compare well with the latent heat value of $5\,Jg^{-1}$ reported for a N_D to N_L transition in a discotic nematic liquid crystal [4].

The occurrence of an endothermic peak on cooling is unusual (Fig. 4). However, inverse (exothermic) DSC peaks are reported for the lower homologue of this compound between the glass and crystal melting transitions on heating and ascribed to structural variations (recrystallization) taking place in these compounds [20]. Even the calamitic nematic liquid crystal 5CB is reported to exhibit an exothermic peak on heating, due to the occurrence of a more stable, additional crystalline phase, which is not observed while cooling the sample [21]. This indicates that the endothermic peak seen in our sample may be due to some structural variations occurring in the N_3 phase.

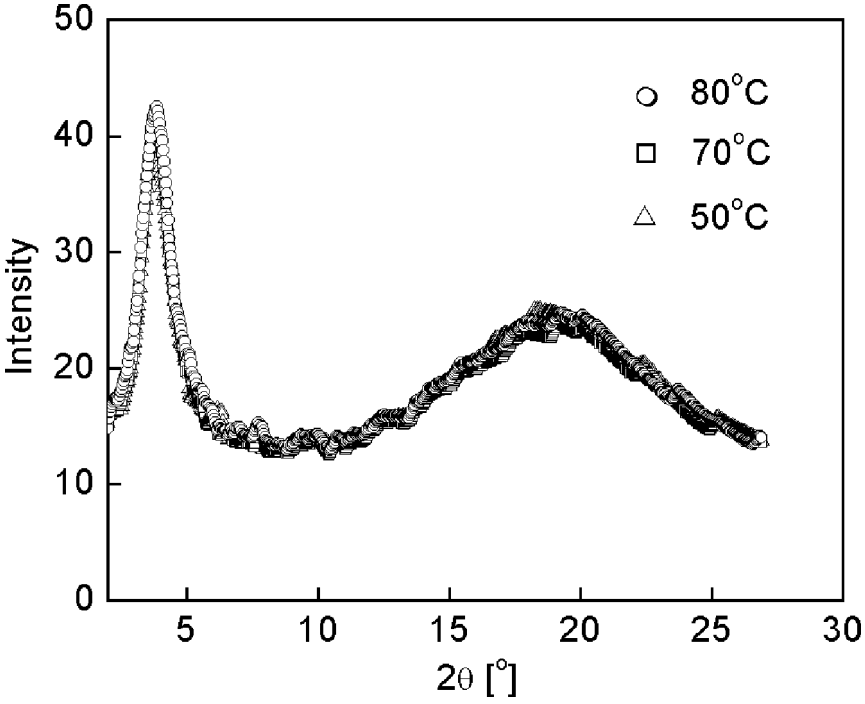

FIGURE 8 XRD pattern of the sample on slow cooling for three different temperatures: 80°C, 70°C, and 50°C.

Some representative textures of N_1, N_2, and N_3 phases can be seen in Fig. 5. The N_1 phase shows schlieren texture along with marble texture. In the N_2 phase only a marble texture is seen. In the onset of the N_3 phase (at 52°C), the marble texture changes to complementary colors with respect to the texture in the N_2 phase.

The temperature dependence of some lateral XRD peaks of N_1, N_2, and N_3 phases are shown in Fig. 10. In each of the N_1, N_2, and N_3 phases, the peak positions are independent of the temperature. The peak positions are 3.88°, 3.79°, and 3.72° for N_1, N_2, and N_3 phases respectively on 2θ scan. However, on comparing the lateral peaks of N_1, N_2, and N_3 phases, we find the peak positions shift toward the lower 2θ values going from N_1 to N_3 phases (Fig. 9). Such a shift in the XRD peaks is reported for a smectic A to smectic C transition due to changes in the layer spacing brought about by the tilting of the molecules [22]. In our case, the observed shifts in the XRD peaks may be due to variations in the lateral distance between the discotic

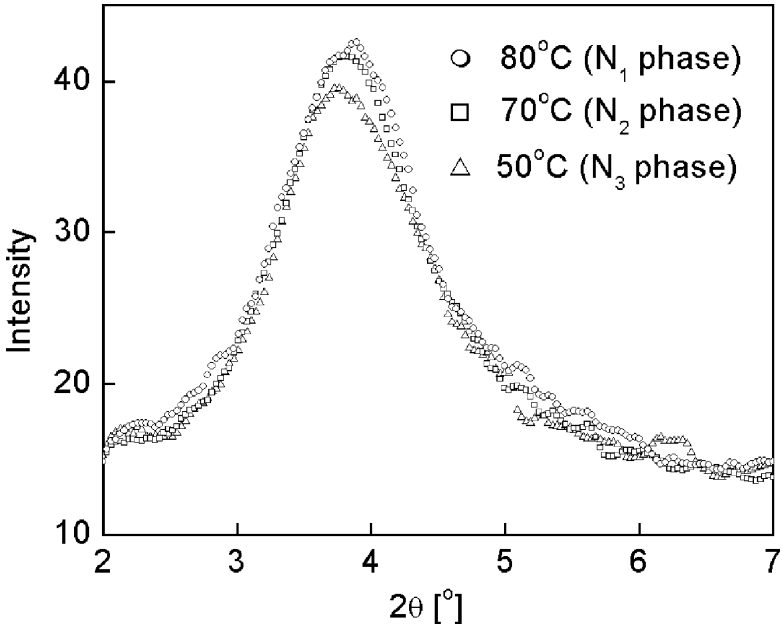

FIGURE 9 Comparison of lateral peaks of N_1, N_2, and N_3 phases.

molecules in the three nematic phases. The lateral distance between the discotic molecules (d_{lat}) calculated from Bragg condition, $2d \sin\theta = \lambda$ [θ is angle of peak position on 2θ scan and λ is wavelength of electromagnetic radiation (1.54 Å)] is shown in Fig. 11. We find abrupt changes in the lateral distance between the discotic molecules at the phase-transition temperatures. We also find the lateral distance increases from 22.69 Å to 23.68 Å on going from N_1 to N_3 phases.

We believe that in the N_3 phase, the increase in the lateral distance between the discotic molecules may involve the tilting of the molecules with respect to the columnar direction. (Such a tilt of the discotic molecules is not expected to change the distance between them in the columnar direction as also seen in our XRD studies.) This tilted molecular organization in the N_3 phase may result in the tilting of the nematic director with respect to that of the N_2 phase and may be responsible for the observed complementary color change in the optical textures (Fig. 5) on going from N_2 to N_3 phases. The possible structural variations inferred from the endothermic DSC peak in the N_3 phase (Fig. 4) may also be due to the proposed tilted molecular organization. Such a nematic–nematic transition involving tilting of the molecules with respect to the columnar axis is reported for a

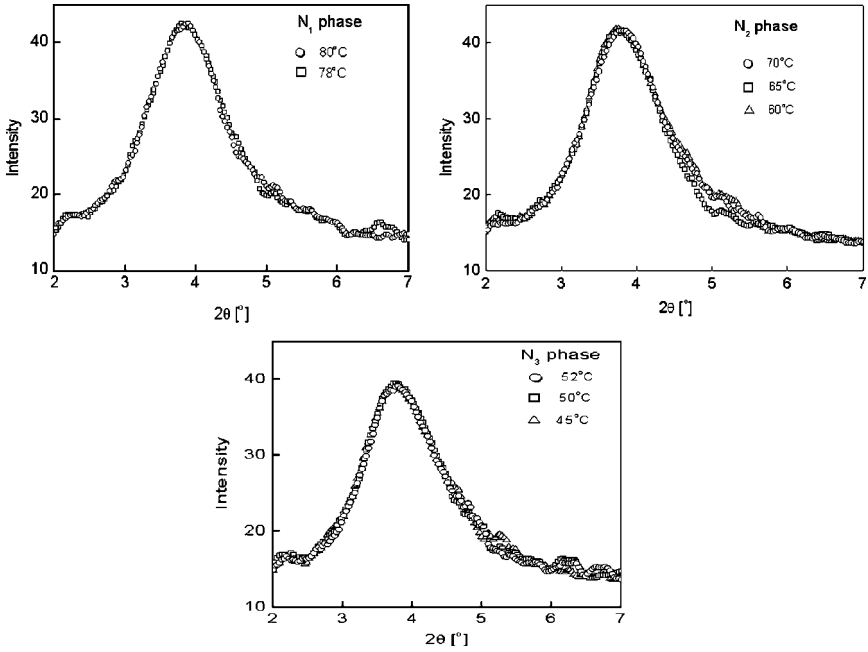

FIGURE 10 Temperature dependence of lateral peaks of N_1, N_2, and N_3 phases.

lyotropic nematic system consisting of sheet-shaped palladium organyls [23]. The proposed model [23] also involves stacking of the sheet-like molecules to give rise to short column-like aggregates without any intra- and intercolumnar molecular order between the aggregates. In our case, the correlation length (ξ) in the columnar direction can be calculated from the width of the columnar XRD reflections by using the relation $\xi = 2\pi/\Delta q$, where $\Delta q = q_1 - q_2 : \mathrm{q}_1 = 4\pi \sin\theta_1/\lambda$; $q_2 = 4\pi \sin\theta_2/\lambda : \theta_1$ and θ_2 are the θ values corresponding to the columnar peak at full width at half maximum (FWHM). The relative correlation length (ξ/d) is a measure for spatial order in terms of the molecular dimensions and indicates an approximate number of discotic molecules in the short-columnar aggregation [4], where d is the distance between the discotic molecules along the columnar direction. In our case, the ξ is about 14.4 Å and the measured d value is about 4.5 Å. This give rise to an ξ/d value of about 3. Our x-ray studies also do not reveal any inter or intra columnar molecular ordering.

Paul et al. studied the nematic order parameter as a function of temperature using optical retardation measurements on a discotic

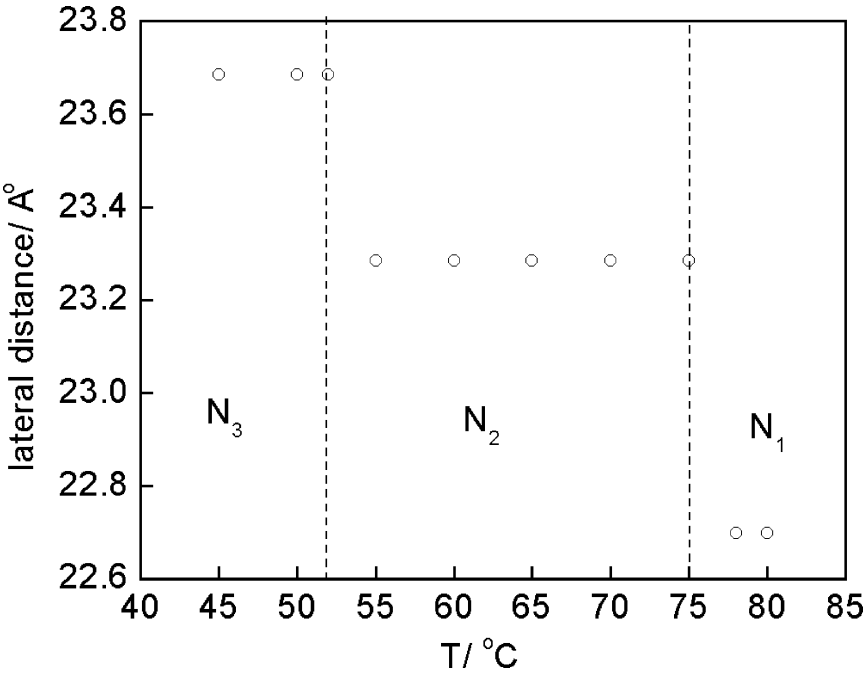

FIGURE 11 Lateral distance between the discotic molecules versus temperature.

nematic liquid crystals exhibiting nematic–nematic transitions [4]. They observed only an inflection point at the transition temperature instead of an expected jump in the order parameter. Assuming that the diamagnetic anisotropy ($\Delta\chi$) is propotional to the nematic order parameter as in the calamitic nematic liquid crystals, we also find only an inflection point at the N_1 to N_2 transition. However, we observed a discontinuous jump at the N_2 to N_3 transition.

Many factors may be responsible for an N-N transition in a nematic liquid crystal. For example, in a highly polar calamitic nematic liquid crystal, a change in the molecular configuration (from a parallel to antiparallel configuration) and a subsequent change in the layer spacings are reported to be responsible for an observed N-N transition [17]. In the case of discotic liquid crystals, the observed N_{Col} and N_L phases are due to the aggregation of discotic molecules in the columnar and lateral directions respectively and a subsequent local nematic ordering. However, the nematic–nematic transitions observed in our sample on slow cooling may be due to the changes in the lateral distance between the molecules as suggested by our x-ray studies.

We find a similar anomaly, but with the transition temperatures slightly shifted as long as we change the cooling rate slowly (<1°C/min). However, we report here only the second cooling of the sample, which involves heating the sample at 0.6°C/min to about 5°C above the isotropic temperature and then cooling it at 0.36°C/min. This enabled us to compare the results of the different techniques adopted to probe these nematic–nematic transitions effectively.

4. CONCLUSIONS

We have carried out thermal, optical, and magnetic studies on a discotic nematic liquid crystal hexakis(4-nonylphenylethynyl)benzene while slowly cooling the sample. We observed anomalous DSC peaks in the nematic region at 75°C and 52°C, which are not observed on fast cooling of the sample. We find discontinuous changes in the mass diamagnetic anisotropy and optical transmission studies at these temperatures, indicating nematic–nematic transitions. We also observed shifts in the lateral XRD peaks in the vicinity of these transitions, which indicate that the changes in the lateral distance between the discotic molecules may be responsible for the observed nematic–nematic transitions.

ACKNOWLEDGMENTS

We are grateful to Prof. V. A. Raghunathan for useful discussions. We thank K. N. Vasudha for DSC measurements and Balakrishnaprabhu for x-ray measurements.

REFERENCES

[1] Praefcke, K., Singer, D., Kohne, B., Ebert, M., Liebmann, A., & Wendorff, J. H. (1991). *Liq. Cryst.*, *10*, 147.
[2] Bengs, H., Karthaus, O., Ringsdorf, H., Baehr, C., Ebert, M., & Wendroff, J. H. (1991). *Liq. Cryst.*, *10*, 161.
[3] Paul, H., Kouwer, J., Jager, W. F., Mijs, W. J., & Picken, S. J. (2000). *Macromolecules*, *33*, 4336.
[4] Paul, H., Kouwer, J., Jager, W. F., van den Berg, O., Mijs, W. J., & Picken, S. J. (2001). *Polymeric Materials: Science & Engineering*, *85*, 303.
[5] Paul, H., Kouwer, J., Jager, W. F., Mijs, W. J., & Picken, S. J. (2001). *Macromolecules*, *34*, 7582.
[6] Praefcke, K. (2001). Physical properties of liquid crystals: Nematics. Dunmur, D. A., Fukuda, A., & Luckhurst, G. R. (Eds.), INSPEC, Hertz, UK, 17.
[7] Cammidge, A. N. & Bushby, R. J. (1998). Handbook of liquid crystals. Demus, D., Goodby, J., Gray, G. W., Spiess, H. W., & Vill, V. (Eds.), Vol. 2B, Chapter VII, Wiley-VCH.

[8] Heppke, G., Ranft, A., & Sabaschus, B. (2003). *Mol. Cryst. Liq. Cryst. Lett.*, *8*, 17.
[9] Kumar, S. & Varshney, S. K. (2000). *Angew. Chem. Int. Ed.*, *39*, 3140.
[10] Kumar, S., Varshney, S. K., & Chauhan, D. (2003). *Mol. Cryst. Liq. Cryst.*, *396*, 241.
[11] Kumar, S. (2003). *Pramana*, *61*, 199.
[12] Kruerke, D., Kitzerow, H. S., Heppke, G., & Vill, V. (1993). *Ber. Bunsenges. Phys. Chem.*, *97*, 1371.
[13] Chandrasekhar, S., Krishna Prasad, S., Nair, G. G., Shankar Rao, D. S., Kumar, S., & Manickam, M. (1999). *EuroDisplay '99, the 19th International Display Research Conference Late-News Papers*, VDE VERLAG GMBH, Berlin, Germany, p. 9.
[14] Yelamaggad, C. V., Prasad, V., Manickam, M., & Kumar, S., (1998). *Mol. Cryst. Liq. Cryst.*, *325*, 33.
[15] Picken, S. J. (1999). Physical properties of liquid crystals: Nematics, Dunmur, D. A., Fukuda, & Luckhurst, G. R. (Eds.), United Kingdom: INSPEC, Hertz, 97.
[16] Dierking, I. (2004). *Textures of liquid crystals*, 53. Wiley-VCH, Weinheim, Germany.
[17] Warrier, S. R., Vijayaraghavan, D., & Madhusudana, N. V. (1998). *Europhys. Lett.*, *44*, 296.
[18] Krishna Prasad, S., Maeda, Y., Shankar Rao, D. S., Nagamani, A., Hiremath, U. S., & Yelamaggad, C. V. (2003). *Liq. Cryst.*, *30*, 1277.
[19] Levelut, A. M. & Hardouin, F. (1981). *J. Physique.*, *42*, 147.
[20] Ebert, M., Jungbauer, D. A., Kleppinger, R., & Wendorff, J. H. (1989). *Liq. Cryst.*, *4*, 53.
[21] Mansare, T., Decressain, R., Gors, C., & Dolganov, V. K. (2002). *Mol. Cryst. Liq. Cryst.*, *382*, 97.
[22] Keum, S. R., Shin, J. T., Lee, S. H., & Shin, S. T. (2004). *Mol. Cryst. Liq. Cryst.*, *411*, 119.
[23] Usol'tseva, N., Haucks, G., Koswig, H. D., Praefcke, K., & Heinrich, B. (1996). *Liq. Cryst.*, *20*, 731.